Am J Transl Res 2021;13(10):11255-11270
www.ajtr.org /ISSN:1943-8141/AJTR0133086

Original Article

Dura cells in the etiopathogenesis of Crouzon syndrome: the effects of FGFR2 mutations in the dura cells on the proliferation of osteoblasts through the hippo/YAP mediated transcriptional regulation pathway

Xin-Hang Dong[1*], Ming-Zi Zhang[2*], Chen-Zhi Lai[1], Cheng-Cheng Li[1], Le Du[1], Guo-Dong Song[1], Xian-Lei Zong[1], Xiao-Lei Jin[1]

[1]*The Sixteenth Department of Plastic Surgery, Plastic Surgery Hospital, Chinese Academy of Medical Sciences & Peking Union Medical College (CAMS & PUMC), Beijing, China;* [2]*Department of Plastic Surgery, Peking Union Medical College Hospital, Beijing, China.* [*]*Co-first authors.*

Received March 12, 2021; Accepted July 12, 2021; Epub October 15, 2021; Published October 30, 2021

Abstract: Background: FGFR2 (fibroblast growth factor receptor 2) mutations are implicated in the etiopathogenesis of syndromic craniosynostosis, and C278F- or C342Y-FGFR2 mutations can lead to Crouzon syndrome. The dura mater exerts crucial effects in the regulation of cranial suture development. However, the underlying mechanisms of these biological processes are rarely studied. This research explored and analyzed the biological function of FGFR2 overexpressed by dura cells on cranial osteoblasts. Methods: Dura cells and cranial osteoblasts from C57BL/6 mice aged 6 days were obtained and cultured respectively. Lentivirus-FGFR2 constructs were engineered with C278F- and C342Y-FGFR2 mutations. The dura cells were infected with the constructs and co-cultured with osteoblasts in a trans-well system. Four experimental groups were established, namely the Oste group, the Oste+Dura-vector group, the Oste+Dura-C278F group, and the Oste+Dura-C342Y group. FACS, CCK8, and EdU assays were used to evaluate the osteoblast proliferation levels. Western blot and RT-qPCR were used to measure the expressions of the factors related to proliferation, differentiation, and apoptosis. Furthermore, the expression levels of the key factors in the Hippo/YAP-PI3K-AKT proliferation pathway were measured and analyzed. Finally, rescue experiments were performed with an RNA interfering assay. Results: The proliferation and differentiation levels of the osteoblasts in the Oste+Dura-C278F and Oste+Dura-C342Y groups were significantly up-regulated, but the apoptosis levels in the four groups were not significantly different. The YAP, TEADs1-4, p-PI3K, and p-AKT1 expressions in the mutant FGFR2 groups were higher than the corresponding expressions in the control groups, and the results of the rescue experiments showed a reverse expression tendency, which further confirmed the effects of the FGFR2 mutations in the dura cells on the proliferation of the osteoblasts and the underlying possible mechanisms. Conclusion: Our studies suggest that the Crouzon mutations (C278F- and C342Y-) of FGFR2 in dura cells can enhance osteoblast proliferation and differentiation and might influence the pathogenesis of craniosynostosis by affecting the Hippo/YAP-PI3K-AKT proliferation signaling pathway.

Keywords: Crouzon syndrome, FGFR2 mutation, dura cells, osteoblasts, underlying mechanisms

Introduction

A type of congenital craniofacial deformity with an incidence of 1/2000-1/2500 [1], craniosynostosis is characterized by the premature fusion of one or more cranial sutures, resulting in cranial malformation and changes in intracranial pressure. Craniosynostosis and its complicated complications have a significant impact on sensory, respiratory, and neurological functions as well as intellectual development [2]. The craniosynostosis mechanism has been extensively studied at the cellular, molecular, and genetic levels, but it is still not fully understood. Further studies on the diagnosis and treatment of the related gene targets in craniosynostosis are particularly crucial and indispensable. According to the severity of the cranial deformity and its complications, craniosynostosis is divided into non-syndromic and syndromic craniosynostosis. Studies have demonstrated that FGFR2 mutations are associated

with a variety of abnormal bone and cartilage formations, and multiple-locus mutations can result in FGFR2 structural activation [3, 4]. Crouzon syndrome is one of the most common clinical types of syndromic craniosynostosis, and it is closely related to the C278F- and C342Y-FGFR2 mutations [3, 5, 6].

It is now generally acknowledged that the physiological development of cranial sutures is related to complex interactions between the brain, the dura mater, and the skull itself. The early closure of the cranial sutures occurs when the biochemical environment and the genetic heredity around the cranial sutures have changed and are accompanied by complex growth and development. More and more studies have shown that dura and dura-derived soluble mediators play an important role in the pathogenesis of craniosynostosis. However, the underlying mechanism of dura-derived FGFR2 secretions in the pathogenesis of Crouzon syndrome remain unclear. The purpose of this study was to analyze the effects of FGFR2-mutated dura cells on the proliferation of co-cultured osteoblasts and the underlying mechanism.

The Hippo pathway, a newly discovered pathway implicated in cell development, proliferation, and differentiation, plays an irreplaceable role in regulating tissue growth, homeostasis, and regeneration [7, 8]. YAP (yes-associated protein) is a key effector of the Hippo pathway, which is regulated by LATS2 (large tumor suppressor-2) and which induces the expression of related target genes by interacting with transcriptional factors such as TEADs (TEA domain transcription factors) 1-4 to exert related biological efficacy [9, 10]. In this study, we evaluated the promoting effects of FGFR2 signaling molecules from the dura on osteoblast proliferation, and we also explored the underlying mechanisms in osteoblastic proliferation regulation with C278F- and C342Y-FGFR2 mutations over-expressed by dura cells. This study provides a theoretical basis for future research.

Methods

Tissue isolation and cell culture

The dura and calvarial bone were harvested from 6-day-old C57BL/6 mice and were carefully dissected. All the operations were conducted in line with the National Institutes of Health's *Guidelines for the Care and Use of Laboratory Animals*. The experiments were performed according to the Experimentation Ethics Committee on Animal Rights Protection of the Chinese Academy of Medical Sciences & Plastic Surgery Hospital (approval number, 2018089). The separated calvarial bone and dura were washed with a PBS (phosphate buffer saline) solution 2-3 times, and then cut into 1 mm × 1 mm pieces, respectively. Trypsin enzymic digestion was used to isolate and culture the calvariae osteoblasts cells (20 minutes). Then, centrifugation was conducted and 0.1% collagenase II was added for 2 hours. Collagenase I (3 mg/ml) was applied to digest the dura cells for 45 minutes, and centrifugation was also conducted. The osteoblasts and dura cells were collected and cultured in α-Modified Eagle Medium (α-MEM, Gibco, USA) with 15% FBS (fetal bovine serum) and penicillin-streptomycin at 37°C and 5% CO_2. Then, the dura cells were stained with vimentin antibody (1:5000, Proteintech, Chicago, USA) by immuno-cytological detection, and the osteogenic characterization was determined using ALP (alkaline phosphatase) staining.

Establishment of the lentivirus-FGFR2 constructs

Dural cells were inoculated into a 24-well plate with 1 × 10^5 cells/well. A prepared lentivirus with mutant FGFR2 constructs was then added to a 250 μl preheated serum-free medium and mixed with dura cells in a 24-well cell culture plate, to establish FGFR2 overexpressing dura cells (C278F-FGFR2 and C342Y-FGFR2), and blank vector (vector) dura cells with no lentivirus-induced FGFR2 mutations were used as the control group in the following experiments. The fluorescence expressions (FITC & DAPI) were measured using confocal microscopy (TCS SP8, Leica, Germany) and the subsequent experiments were performed 72-96 hours after infection.

Trans-well co-culture system and grouping

A co-culture system was established where the dura cells could exert a biological impact on the osteoblasts, which was consistent with the organic environment *in vivo* as much as possible. The osteoblasts were planted in the upper chamber, and the dura cells in the lower cham-

Table 1. The dilution ratios and sources for the antibodies in the western blot assays

Antibody	Dilution Ratio	Source
anti-PCNA	1:2000	Proteintech, Chicago, USA
anti-ALP	1:1000	Proteintech, Chicago, USA
anti-RUNX2	1:1000	abcam, Cambridge, UK
anti-Osteopontin	1:1000	Proteintech, Chicago, USA
anti-Osteocalcin	1:1000	abcam, Cambridge, UK
anti-pro-caspase3	1:1000	abcam, Cambridge, UK
anti-cleaved-caspase3	1:500	abcam, Cambridge, UK
anti-YAP	1:5000	abcam, Cambridge, UK
anti-p-YAP	1:1000	abcam, Cambridge, UK
anti-p-PI3K	1:1000	abcam, Cambridge, UK
anti-AKT	1:500	abcam, Cambridge, UK
anti-p-AKT	1:1000	abcam, Cambridge, UK
anti-GAPDH	1:20000	Proteintech, Chicago, USA
anti-β-actin	1:5000	Proteintech, Chicago, USA

ber could affect the osteoblasts due to the permeability of the polycarbonate membrane, to study the effects of FGFR2 secreted by the dura cells on the performance of osteoblasts.

Four different groups were set up in this study, two control groups of isolated osteoblasts (Oste) and co-cultured osteoblasts with no lentivirus-induced FGFR2 mutation (Oste+Dura-vector), and two co-cultured groups with FGFR2 overexpressions (Oste+Dura-C278F and Oste+Dura-C342Y).

EdU (5-ethynyl-2'-deoxyuridine) assay

A BeyoClick™ EdU Cell Proliferation Kit with Alexa Fluor 555 (Beyotime, Shanghai, China) was performed following the manufacturer's instructions. Appropriate numbers of four different groups of cells were cultured in 96-well plates, and the cells were cultured overnight. 2 × EdU working solution was prepared and added into 96-well plates in equal proportions. EdU labeled cells were harvested and 1 ml fixation solution was added at room temperature for 15 minutes. 0.5 ml Click Reaction Solution was then added to each well and co-incubated at room temperature for 30 minutes.

Cell proliferation analysis

To further evaluate the cell proliferation capabilities, the proliferation index of the osteoblasts in four groups was examined using the CCK-8 (Cell Counting Kit-8, GLPBIO, USA) method by utilizing highly water-soluble tetrazolium salt. The osteoblasts were seeded in a 96-well plate and cultured. 10 μl of CCK-8 solution was added to the 96-well plate and mixed gently on an orbital shaker. A microplate reader was used to measure the absorbance at 450 nm.

Cell cycle examination

In the cell cycle analysis experiments, the osteoblasts were digested with trypsin, and the cell culture medium collected in the centrifuge tubes was added. The adherent cells were blown down and gently blown away. Then, the osteoblasts were fixed in 70% ethanol at 4°C for 12 hours. Then, the cell precipitation was resuspended slowly and stored at 4°C. The fluorescence was measured using flow cytometry at the excitation wavelength of 488 nm and the light scattering was also measured. FlowJo 10.7.1 was used for the DNA content and light scattering analyses.

Western blot

After the osteoblasts of the logarithmic growth phase were treated according to the experimental protocol, the cells were scraped off the petri dish with a cell scraper and collected into a 15 mL centrifuge tube for centrifugation. Lysis and centrifugation were then performed. Different materials were carefully placed into the transfer film buffer, according to the prescribed sequence. The samples were stained with an appropriate dilution of primary antibodies (**Table 1**) at 4°C for twelve hours. The membranes were incubated at 37°C with secondary antibodies of a recommended dilution for 1 hour, and color determination was performed.

RNA isolation and RT-qPCR

The RNA from the different samples was extracted using TRIzol™ Reagent, following the manufacturer's instructions. The RNA quality was measured using the ultraviolet absorption method. The forward and reverse primers are shown in **Table 2**, and the GAPDH was set for normalization. cDNA was synthesized, the primer specificity was detected, and an RT-qPCR reaction system was established. Then, PCR amplification was conducted.

Table 2. The sequences of the primers used for the quantitative real-time PCR

Target gene	Forward	Reverse
FGFR2	5'-CCTCGATGTCGTTGAACGGTC-3'	5'-CAGCATCCATCTCCGTCACA-3'
PCNA	5'-TTTGAGGCACGCCTGATCC-3'	5'-GGAGACGTGAGACGAGTCCAT-3'
CDK1	5'-AGAAGGTACTTACGGTGTGGT-3'	5'-GAGAGATTTCCCGAATTGCAGT-3'
CDK2	5'-CCTGCTTATCAATGCAGAGGG-3'	5'-TGCGGGTCACCATTTCAGC-3'
ALP	5'-GAGCGTCATCCCAGTGGAG-3'	5'-TAGCGGTTACTGTAGACACCC-3'
Runx2	5'-GACTGTGGTTACCGTCATGGC-3'	5'-ACTTGGTTTTTCATAACAGCGGA-3'
Osteopontin	5'-ACCCAGAAACTGGTCATCAGC-3'	5'-CTGCAATACACACACTCATCACT-3'
Osteocalcin	5'-CTGACCTCACAGATCCCAAGC-3'	5'-TGGTCTGATAGCTCGTCACAAG-3'
LATS2	5'-GGACCCCAGGAATGAGCAG-3'	5'-CCCTCGTAGTTTGCACCACC-3'
YAP	5'-TACTGATGCAGGTACTGCGG-3'	5'-TCAGGGATCTCAAAGGAGGAC-3'
TEAD1	5'-AAGCTGAAGGTAACAAGCATGG-3'	5'-GCTGACGTAGGCTCAAACCC-3'
TEAD2	5'-GAAGACGAGAACGCGAAAGC-3'	5'-GATGAGCTGTGCCGAAGACA-3'
TEAD3	5'-CAACCAGCACAATAGCGTCCA-3'	5'-CTGAAAGCTCTGCTCGATGTC-3'
TEAD4	5'-CAACCTGGAACATCCCACGAT-3'	5'-GAAAGCCGAGAACTCCAACAT-3'
GAPDH	5'-AGGTCGGTGTGAACGGATTTG-3'	5'-TGTAGACCATGTAGTTGAGGTCA-3'

Knockdown of FGFR2 or YAP via siRNA

Small interfering RNA (siRNA)-involved FGFR2 or YAP knockdown experiments were performed according to the manufacturer's instructions. In brief, 20 pmol of well-designed siRNA was added into serum-free α-MEM and mixed gently. 1 ul Lipofectamine™ 2000 (ThermoFisher SCIENTIFIC) reagent was added to another 50 ul serum-free medium. Lipofectamine™ 2000 reagent was mixed with siRNA and then added to the cell culture medium and incubated in a CO_2 incubator, followed by the subsequent experiments.

Statistical analysis

In this study, the experimental data analysis was conducted with SPSS 26.0 and GraphPad Prism 8. The data were shown as the means ± SD (means ± standard deviation), and one-way analyses of variance (ANOVA) were applied. Statistical significance was set at $P<0.05$.

Results

Identification and characterization of the dura cells and osteoblasts

In our study, the morphologies of the dura cells and osteoblasts cells were observed using phase-contrast microscopy and displayed a spindle-shaped "fibroblast" appearance. The dura cells showed a strong positive reaction to vimentin, and the staining area was mainly located in the cytoplasms [11]. Vimentin is specifically expressed in fibroblasts, vascular endothelial cells, and other cells derived from mesenchyme. In our study, the dura cells stained positively with anti-vimentin in the cytoplasms, and the osteoblasts showed positive staining with alkaline phosphatase (**Figure 1**).

Verification of the dura calls infected with the FGFR2 genes

To examine the expression of the virally induced FGFR2 in the dura cells infected with FGFR2 point mutation genes (Dura-C278F and Dura-C342Y), immunofluorescent staining was performed in this study. The results indicated that the expression of FGFR2 was higher in the Dura-C278F cells and Dura-C342Y cells compared with the dura cells without virally induced FGFR2 (**Figure 1**).

Evaluation of the proliferative capability of the osteoblasts co-cultured with dura cells

The effects of the FGFR2 overexpression on the cell cycle of the osteoblasts were evaluated using FACS (fluorescence-activated cell sorting) (**Figure 2**). In the Oste+Dura-C278F and Oste+Dura-C342Y groups, (43.01±0.82)% and (44.41±1.03)% of cells were in the G0/G1 phase, (29.47±1.18)% and (28.6±0.64)% were in the S phase, and (27.64±0.34)% and (27.03±1.66)% were in the G2/M phase. The

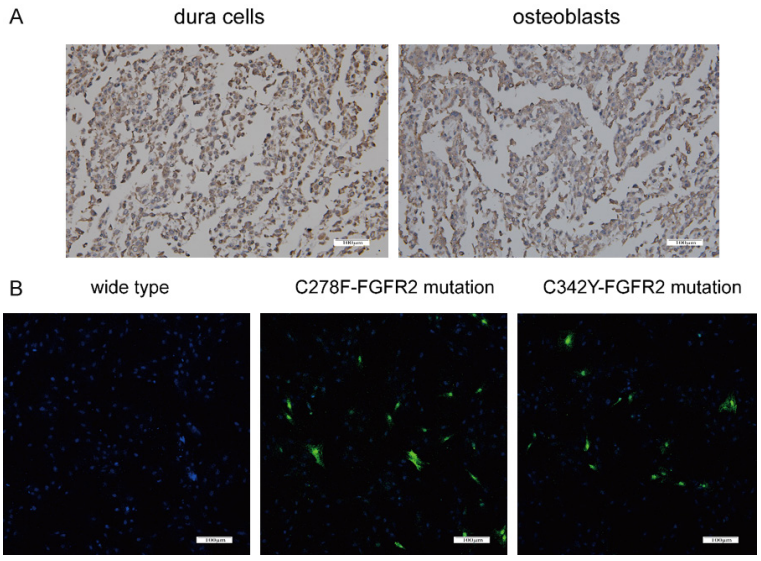

Figure 1. Detection of the dura cells and osteoblasts, and the validation of the virally induced FGFR2 expressions in the dura cells. A. Based on a strong positive reaction to vimentin, the dura cells were positively stained with vimentin antibodies in the cytoplasms using immunocytological detection. The osteogenic differentiation was detected through ALP (alkaline phosphatase) staining, which was a general method for osteoblast detection. B. Virally induced FGFR2 expression in the dura cells measured using confocal microscopy, that were dura cells without virally induced FGFR2 (the wide type), dura cells with the C278F-FGFR2 mutation, and dura cells with the C342Y-FGFR2 mutation.

percentages of the osteoblasts in the S phase of the Oste+Dura-C278F and the Oste+Dura-C342Y groups were higher than they were in the Oste and Oste+Dura-vector groups ($P< 0.05$). Similarly, compared with the osteoblasts in the Oste and Oste+Dura-vector groups, the percentages of osteoblasts in the G2/M phase of the FGFR2 overexpressed groups were also up-regulated ($P<0.05$). In addition, the osteoblasts in the Oste+Dura-C278F and Oste+Dura-C342Y groups had a reduction in the G0/G1 phase ($P<0.05$).

Based on the FACS findings, the FGFR2 overexpression improved the osteoblast percentages in the S and G2/M phases. CCK-8 experiments were further performed to examine the effects of overexpressed FGFR2 on the proliferative abilities of the osteoblasts co-cultured with dura cells (**Figure 2**). The results indicated that the proliferation indexes of the osteoblasts in the Oste+Dura-C278F and the Oste+Dura-C342Y groups were significantly higher than they were in the Oste or Oste+Dura-vector groups, and they showed a time-dependent increasing tendency.

EdU staining was also performed to evaluate the osteoblast proliferation. In this assay, EdU can be used to measure the newly synthesized osteoblast DNA, double-labeled with cell nuclear markers (DAPI) to measure the cell proliferation rate, which could be used for a comprehensive analysis of the cell localization and qualitative determination. The results showed that the osteoblast proliferation levels in the Oste+Dura-C278F and Oste+Dura-C342Y groups were higher than they were in the Oste and Oste+Dura-vector groups in terms of the qualitative detection (**Figure 2**).

PCNA (Proliferating Cell Nuclear Antigen), a homotrimer, is a crucial accessory protein for DNA polymerase δ [12] and is an important indicator for evaluating cell proliferation [13, 14]. Additionally, CDK1 and CDK2 play a crucial role in the regulation of the cell cycle as key proteins promoting cell proliferation. According to the western blot and RT-qPCR, PCNA results, the CDK1, and CDK2 expressions in the osteoblasts in the Oste+Dura-C278F and Oste+Dura-C342Y groups were significantly higher than they were in the other two groups (**Figure 3**). The above results demonstrate that FGFR2 overexpression can up-regulate the proliferative ability of osteoblasts co-cultured with dura cells.

Differentiation capability evaluation of the osteoblasts co-cultured with dura cells

ALP, RUNX2, osteopontin, and osteocalcin are crucial indicators used to evaluate the osteoblast differentiation levels. In this experiment, the expression levels of these four factors were measured with western blot and RT-qPCR assays. The ALP, RUNX2, osteopontin, and osteocalcin proteins showed higher expression levels in the Oste+Dura-C278F and Oste+Dura-C342Y groups than in the other groups, as was visualized in the western blot images (**Figure 3**). Further measurements were per-

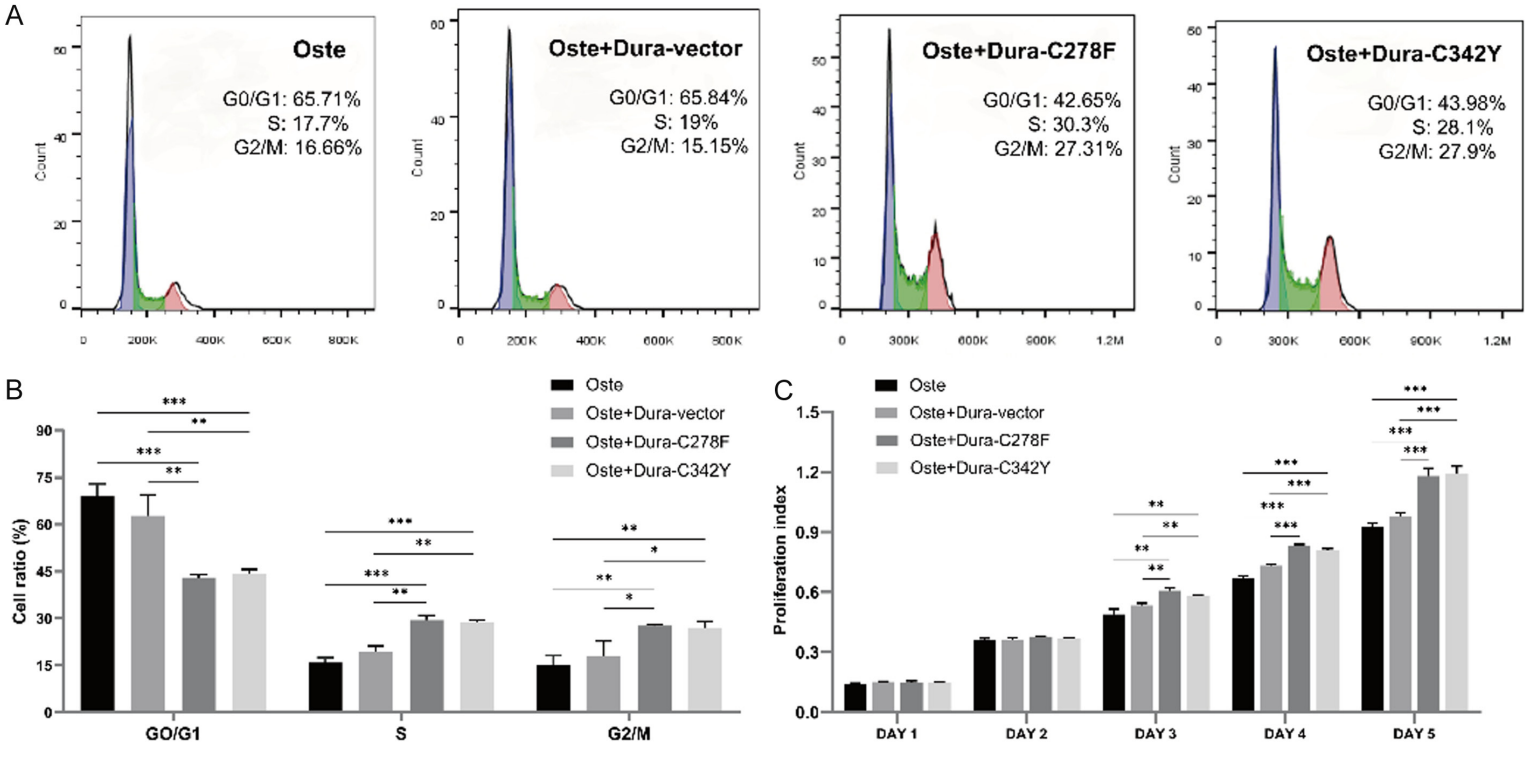
A
Oste
G0/G1: 65.71%
S: 17.7%
G2/M: 16.66%
Oste+Dura-vector
G0/G1: 65.84%
S: 19%
G2/M: 15.15%
Oste+Dura-C278F
G0/G1: 42.65%
S: 30.3%
G2/M: 27.31%
Oste+Dura-C342Y
G0/G1: 43.98%
S: 28.1%
G2/M: 27.9%
Count
B
Oste
Oste+Dura-vector
Oste+Dura-C278F
Oste+Dura-C342Y
Cell ratio (%)
GO/G1
S
G2/M
C
Proliferation index
DAY 1
DAY 2
DAY 3
DAY 4
DAY 5

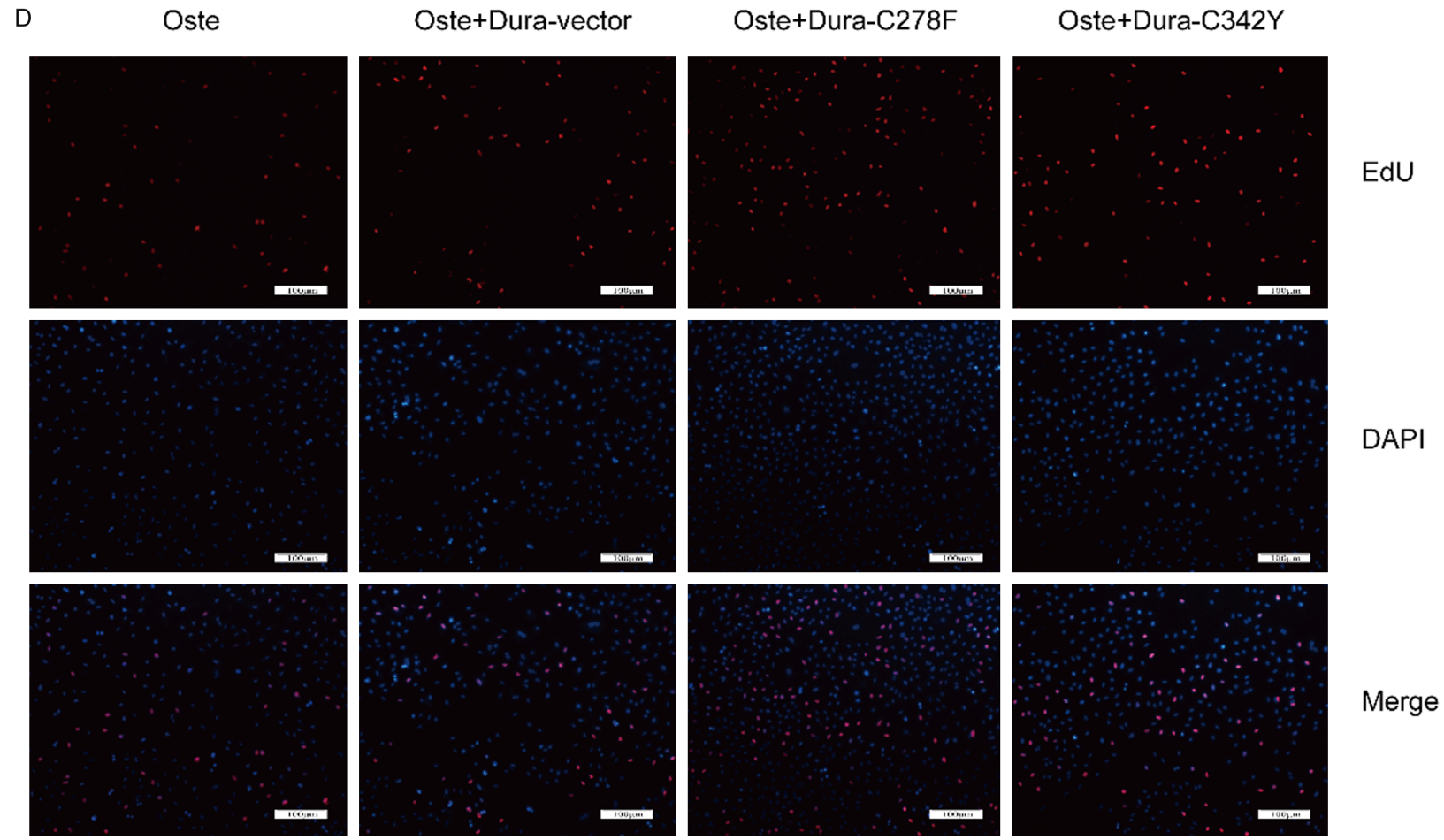

Figure 2. The effects of the FGFR2 overexpression on the proliferation capacities of the osteoblasts co-cultured with dura cells. A. Evaluation of the cell cycle in the different groups using FACS. B. Different phases of the cell cycle in the Oste, Oste+Dura-vector, Oste+Dura-C278F, and Oste+Dura-C342Y groups. C. A CCK-8 assay was further performed to evaluate the osteoblast proliferation index (day 1 to day 5). D. Representative immunofluorescence micrographs of EdU staining visually showed the overall proliferation levels of the osteoblasts in the different groups. The red color showed the EdU positive staining of the proliferating cells, and the blue color showed the cell nuclei stained with DAPI. The percentages of positive cells with EdU staining were: 50.2443±13.4780 (Oste), 53.6011±15.3552 (Oste+Dura-vector), 78.8621±8.4261 (Oste+Dura-C278F), and 82.1183±14.8147 (Oste+Dura-C342Y), which had significant differences (Oste+Dura-C278F vs. Oste, $P<0.05$, Oste+Dura-C342Y vs. Oste, $P<0.05$). The values were measured as the means ± SD, $^{*}P<0.05$, $^{**}P<0.01$, $^{***}P<0.001$.

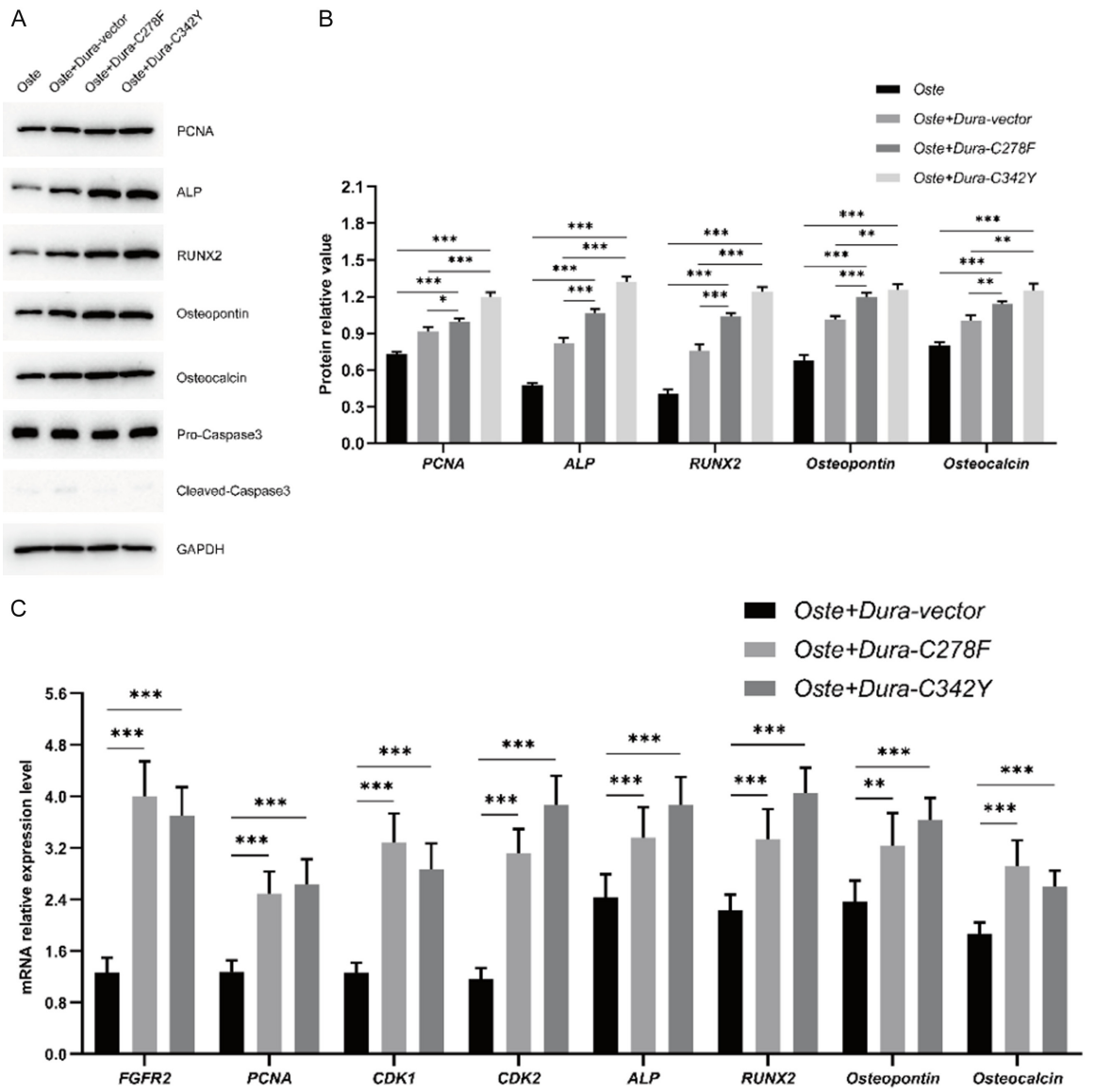

Figure 3. The FGFR2, PCNA, CDK1, CDK2, ALP, RUNX2, Osteopontin, Osteocalcin, and Caspase3 expression levels. A. Representative images of the western blots for PCNA, ALP, RUNX2, Osteopontin, Osteocalcin, and Caspase3 (pro- and cleaved-caspase3). B. Densitometric analyses of the PCNA, ALP, RUNX2, Osteopontin, and Osteocalcin proteins. C. Detection of the FGFR2, PCNA, CDK1, CDK2, ALP, RUNX2, Osteopontin and Osteocalcin mRNA were performed using RT-qPCR. The values were measured as the means ± SD, $^{*}P<0.05$, $^{**}P<0.01$, $^{***}P<0.001$.

formed using RT-qPCR, and the results were consistent with western blot. The mRNA relative values of the above genes were more significantly up-regulated in the Oste+Dura-C278F and Oste+Dura-C342Y groups than in the other two groups.

Mechanism analysis of the effects of the FGFR2 overexpression in the dura cells

After binding to the FGFs ligand, FGFR2 dimerizes and activates the tyrosine kinase activity of the FGFR2 intracellular segments, transmitting signals downstream through a variety of signaling pathways, including the PI3K-AKT signaling pathway, which is closely related to cell proliferation [15, 16]. In addition, a growth inhibition signaling pathway, the Hippo signaling pathway plays a complex regulatory role in biological processes such as cell proliferation, differentiation, and senescence.

In this study, the LATS2, p-YAP, YAP, TEADs1-4, p-PI3K, AKT1, and p-AKT1 expressions were

quantified and analyzed using western blot and RT-qPCR. Compared with of the Oste and Oste+Dura-vector groups, the YAP, TEADs1-4, p-PI3K, and p-AKT1 proteins were expressed at higher levels in the Oste+Dura-C278F and Oste+Dura-C342Y groups, but the LATS2 and p-YAP expressions were lower in these two groups (**Figure 4**). The AKT1 expression was not significantly different in the four groups. The results demonstrated that FGFR2 overexpression is closely related to the upregulation of the key genes in the Hippo/YAP-PI3K-AKT pathway that improve the osteoblast proliferation levels.

YAP-siRNA in osteoblasts co-cultured with dura cells

We performed a rescue experiment with an RNA interfering assay (YAP-siRNA) on the osteoblasts. The osteoblasts were co-cultured with Dura-C278F and Dura-C342Y, respectively. Different groups of osteoblasts with no other treatments (Oste), with non-targeting control siRNA (Oste+blank-vector), and with YAP-siRNA (Oste+siRNA) were used in this experiment. The western blot results showed that the YAP, p-PI3K, and p-AKT1 expressions were significantly down-regulated in the Oste+siRNA group, compared with the Oste and Oste+blank-vector groups (**Figure 4**), demonstrating that down-expressed YAP in osteoblasts has an inhibitory effect on the p-PI3K and p-AKT1 expressions.

The ubiquitin-proteasome pathway and YAP degradation

Current research shows that the phosphorylation modification of YAP is one of the main post-translational modification pathways leading to the degradation of its activity. At the same time, similar studies have found that ubiquitination also participates in the modification of the YAP protein and regulates its activity [17]. The ubiquitin-proteasome pathway is the main degradation process of ubiquitinated substrates. To explore whether the proteasome plays a role in the degradation of YAP, we introduced the proteasome inhibitor MG132 to determine the YAP expression level. Different groups of osteoblasts with no other treatments (Oste), non-targeting control siRNA (Oste+blank-vector), YAP-siRNA (Oste+siRNA), and YAP-siRNA+MG132 (Oste+siRNA+MG132) were used in this experiment. The western blot results showed that the down-regulation of YAP expression was significantly alleviated with the treatment of MG132 (**Figure 5**).

The effects of FGFR2-siRNA on the proliferation ability of osteoblasts co-cultured with dura cells

To further explore the effects of FGFR2 overexpression in dura cells on the biological function of osteoblasts in co-culture experiments, we performed a rescue experiment with an RNA interfering assay (FGFR2-siRNA) of the dura cells (Dura-siRNA). RT-qPCR was used to evaluate the FGFR2 expression levels in the dura cells after the RNA interfering experiments. Dura cells treated with no other treatments (Dura) and cells treated with non-targeting control siRNA (Dura-control) were used in the experiment. Then, the dura cells in the three groups were co-cultured with osteoblasts, respectively, and the proliferative abilities of the osteoblasts at the different time points and in the different groups (Oste+Dura, Oste+Dura-control, and Oste+Dura-siRNA) were detected and measured by the CCK8 experiment. The results showed that, compared with the Oste+Dura and Oste+Dura-control groups, the proliferative ability of the Oste+Dura-siRNA group was significantly inhibited, further demonstrating that the FGFR2 secreted by dura cells can promote the proliferation of co-cultured osteoblasts. In addition, we conducted western blot and RT-qPCR experiments, and the results showed that the YAP, TEADs1-4, p-PI3K, and p-AKT1 expressions were significantly down-regulated in the Oste+Dura-siRNA group, but the LATS2 and p-YAP expressions were up-regulated (**Figure 5**), verifying the underlying mechanisms of FGFR2 secreted by the dura cells to promote the proliferative abilities of the co-cultured osteoblasts.

Discussion

Crouzon syndrome is a type of syndromic craniosynostosis characterized by severe craniofacial deformities and caused by the premature closure of cranial sutures. This disease not only has a serious impact on appearance but can also lead to delayed brain development, causing serious neurological and psychological disorders. The gene mutation in most Crouzon syndrome cases is closely associated with

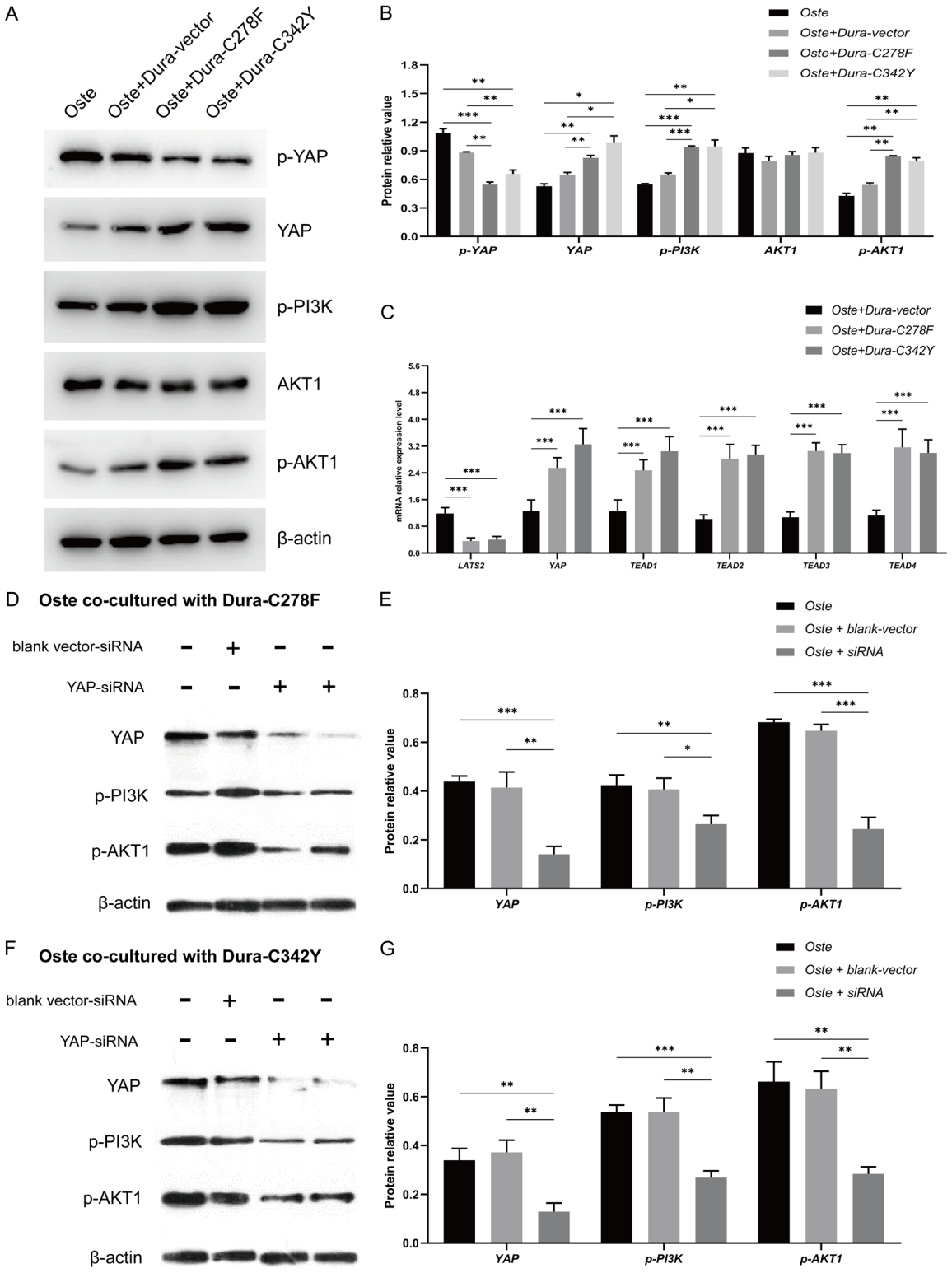

Figure 4. The LATS1, p-YAP, YAP, TEADs1-4, p-PI3K, AKT1, and p-AKT1 expression levels. A. Representative images of western blots for p-YAP, YAP, p-PI3K, AKT1 and p-AKT1. B. Densitometric analyses of p-YAP, YAP, p-PI3K, AKT1 and p-AKT1. C. The quantifications of LATS1, YAP and TEADs1-4 mRNA were performed using RT-qPCR. Rescue experiments. D-G. The effects of YAP-siRNA on the expression levels of p-PI3K and p-AKT1 of the osteoblasts in different groups. The expression levels of the YAP, p-PI3K and p-AKT1 proteins were measured and analyzed using western blot with a densitometric analysis. Values were measured as the means ± SD, $^{*}P<0.05$, $^{**}P<0.01$, $^{***}P<0.001$.

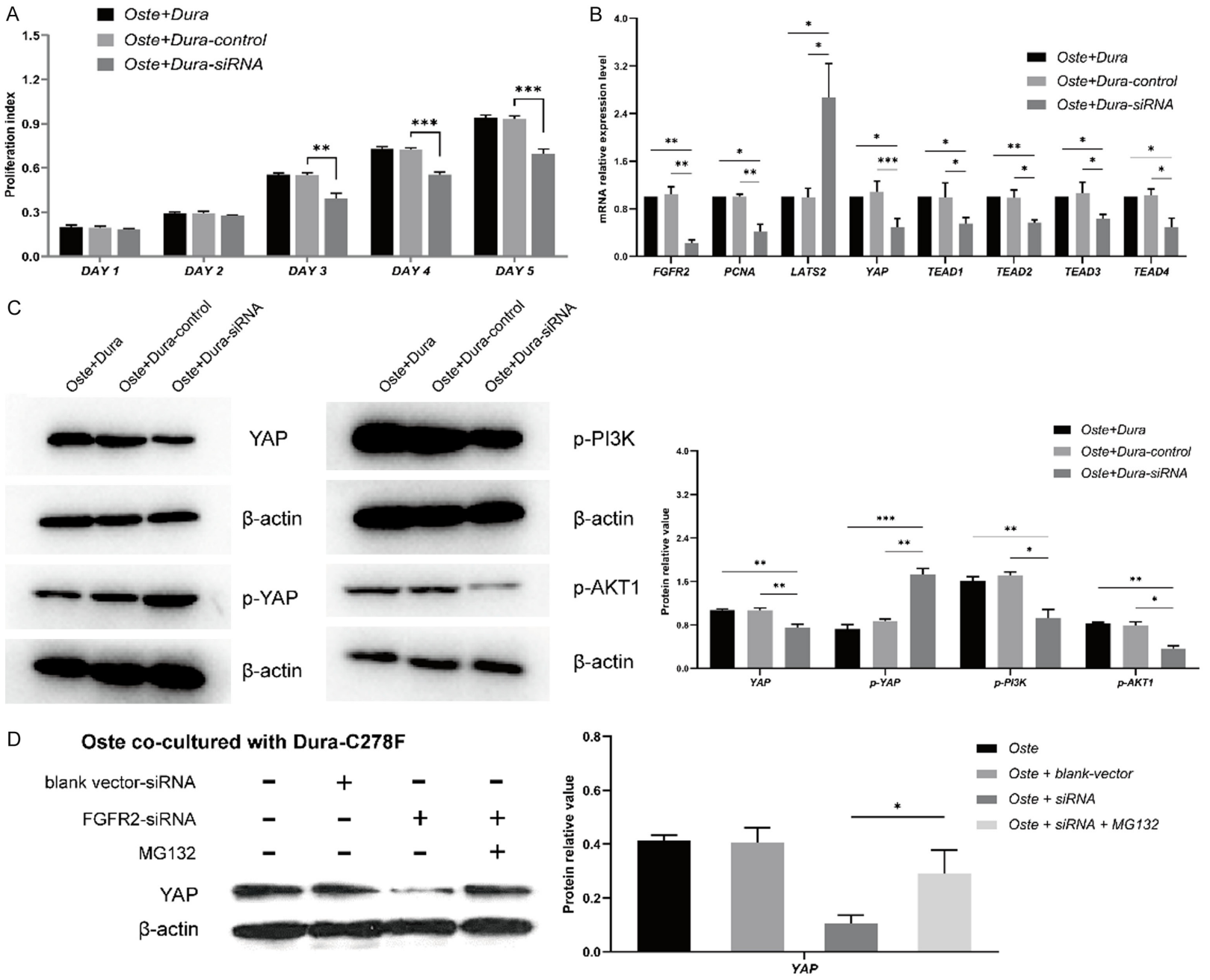
A
Oste+Dura
Oste+Dura-control
Oste+Dura-siRNA
Proliferation index
DAY 1
DAY 2
DAY 3
DAY 4
DAY 5
B
mRNA relative expression level
FGFR2
PCNA
LATS2
YAP
TEAD1
TEAD2
TEAD3
TEAD4
C
YAP
β-actin
p-YAP
p-PI3K
p-AKT1
Protein relative value
D
Oste co-cultured with Dura-C278F
blank vector-siRNA
FGFR2-siRNA
MG132
Oste
Oste + blank-vector
Oste + siRNA
Oste + siRNA + MG132

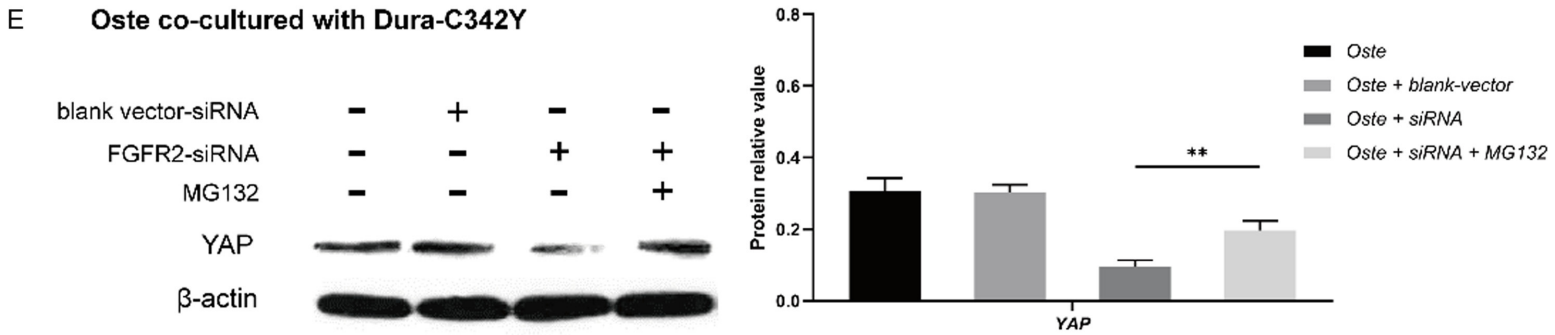

Figure 5. The effects of FGFR2-siRNA on the biological functions of the osteoblasts. A. The effects of FGFR2-siRNA on the proliferation capacities of the osteoblasts in the different groups. B. The quantifications FGFR2, PCNA, LATS1, YAP, and TEADs1-4 mRNA were performed using RT-qPCR. C. The p-YAP, YAP, p-PI3K and p-AKT1 protein expression levels were measured and analyzed using western blot with a densitometric analysis. Studies on the degradation of YAP in the proteasome pathway. D, E. The YAP protein expression levels were measured and analyzed using western blot with a densitometric analysis. The results are presented as the means ± SD, $^{*}P<0.05$, $^{**}P<0.01$, $^{***}P<0.001$.

the FGFR2 gene located on chromosome 10, and it plays a crucial role in regulating the growth and development of craniofacial bones [18]. Mutations in the FGFR2 gene may reduce the stability of the immunoglobulin structure by affecting the conserved amino acid residues at the edge of the Ig III domain, leading to the ligand-independent dimerization and activation of multiple downstream signaling pathways [19]. This pathological process is associated with the pathogenesis of Crouzon syndrome. Furthermore, most of these mutations are missense mutations, including Cys278Phe and Cys342Tyr (C278F- and C342Y-) of the FGFR2 mutations, leading to a constitutive activation of the signaling receptors and pathways [3, 20].

More and more studies have shown that dura mater, the dense fibrous membrane below the cranial bones, provides crucial regulatory signals for the physiological closure of the cranial sutures and the growth and development of the cranial cavity [21-23]. There is only one study that has assessed the effects of FGFR2 point mutation in the dura cells on the proliferation and differentiation of osteoblasts via paracrine [6]. In Ang's study, immature dura cells were transfected with lentivirus to form an FGFR2 gene mutation model, the same as the FGFR2 mutant phenotype found in patients with Crouzon syndrome. An MTT assay showed that the osteoblasts' proliferation levels could be improved by a co-culturing of the osteoblasts and dura cells transfected with the FGFR2 mutation [6]. However, there is a tremendous lack of knowledge of the molecular mechanisms and a lack of in vitro studies evaluating the pathological biology of dura cells and osteoblasts based on the Crouzon model.

The Hippo signaling pathway is a kinase chain composed of a series of protein kinases and transcription factors, and it plays an important and indispensable role in the occurrence and development of a variety of diseases [7, 24]. The Hippo pathway is widely involved in the regulation of the physiological functions and pathological processes of the human body, and it acts as a "checkpoint" in the regulation of moderate development, regeneration, and growth [25, 26]. The key factors associated with the Hippo pathway, such as LATS2, YAP and TEADs1-4, interact with other signaling pathways through different mechanisms in the process of cell proliferation and programmed cell death regulation, thus forming a complex signaling network [27]. In our preliminary experiments, verteporfin, a YAP inhibitor, was applied to osteoblasts co-cultured with C278F-FGFR2 dura cells, and the proliferation of osteoblasts was significantly down-regulated compared to a control group. Therefore, we speculated that the Hippo pathway shaped a "traffic junction" with other signaling pathways related to proliferation regulation in the pathological process of Crouzon syndrome, including the PI3K-AKT pathway, an important cell proliferation pathway affected by FGFR2 activation. YAP acts as a bridge of signaling communication and mediates multiple cell signals to regulate osteoblastic proliferation through the PI3K-AKT pathway (**Figure 6**).

Our study evaluated and confirmed the theory that the dura mater plays a crucial role in the growth and differentiation of osteoblasts. With FGFR2 overexpression constructs, we systematically studied the effects of the FGFR2 point mutations (C278F- and C342Y-) in dura cells on the proliferation and differentiation of co-cultured osteoblasts. With PCNA quantification, FACS and EdU experiments, we found that the Crouzon (C278F- and C342Y-) mutations in the dura cells enhanced osteoblastic proliferation in a trans-well system. Additionally, the CCK8 assays showed that the proliferative abilities of the co-cultured osteoblasts increased gradually as time went on. The results suggest that the FGFR2 secreted by the dura mater might accelerate suture fusion by increasing the number of osteoblasts at the suture area. Furthermore, we explored and examined the underlying regulatory mechanisms of osteoblast proliferation. The PI3K-AKT pathway exerts important effects on cell proliferation, the cell cycle, and cell metabolism, and is able to co-regulate cell proliferation and programmed cell death together with the Hippo/YAP signaling pathway [28]. Studies have shown that YAP can promote the proliferation of rat cardiomyocytes by activating the PI3K-AKT signaling pathway in vivo [29]. The protein or mRNA expression levels of LATS2, p-YAP, YAP, TEADs1-4, p-PI3K, AKT1 and p-AKT1 were evaluated in our study, and the results showed that the YAP, TEADs1-4, p-PI3K, and p-AKT1 expression levels in the Oste+Dura-C278F and Oste+Dura-C342Y groups were significantly increased, but the LATS2 and p-YAP expressions were decreased, suggesting that the promotion

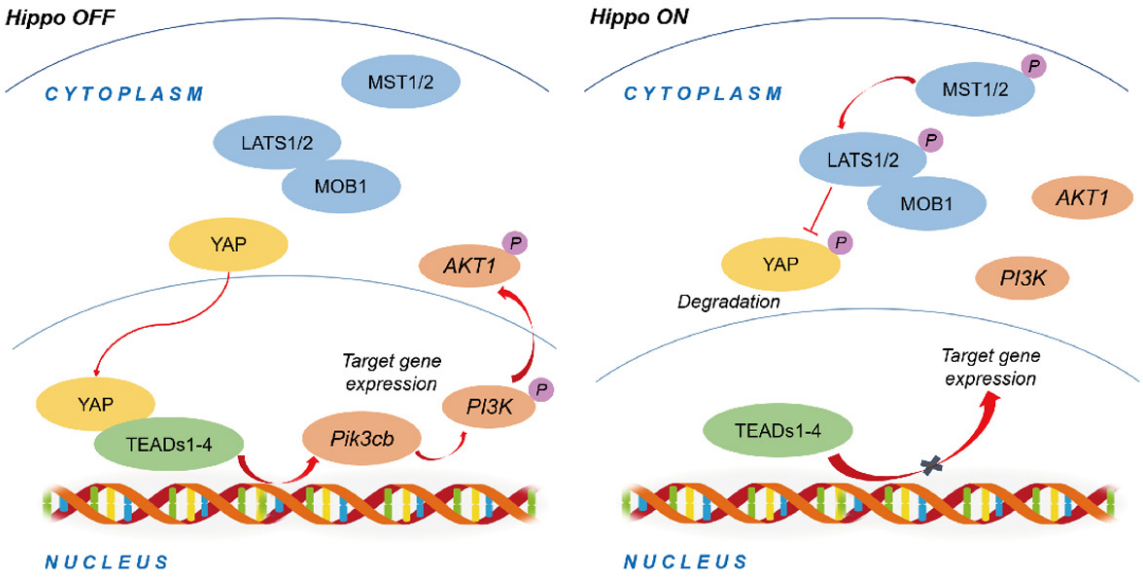

Figure 6. Hippo signaling pathway. The Hippo/YAP pathway was mainly mediated by the phosphorylation levels of multiple key proteins. As shown in the figure above, when the Hippo pathway is "OFF", the translocation of non-phosphorylated YAP binds to the transcription factor TEADs1-4 to form a transcription complex, which activates the target genes including Pik3cb, promoting cell proliferation and differentiation. When the Hippo pathway is "ON", MST1/2 (mammalian sterile20-like kinase 1/2) is initially phosphorylated, which activates LATS1/2 and MOB1 (mps one binder kinaseactivator-like1), and further promotes YAP phosphorylation. Finally, the phosphorylated YAP is modified by ubiquitination and degraded in the cytoplasms.

effects of FGFR2 over-secreted by the dura cells on the osteoblast proliferation were closely related to the Hippo/YAP-PI3K-AKT pathway. When the Hippo pathway is "OFF", the non-phosphorylated YAP binds to the transcription factor TEAD after nuclear translocation to form a transcription complex, activating the relevant target genes and promoting cell proliferation [30]. To further verify our experimental results and hypotheses, we conducted a rescue experiment. The siRNA results showed that the expression levels of these factors showed a reverse tendency after the RNA interfering assay, indicating the close interaction between the FGFR2 expression and the key factors of the above pathway. The ubiquitin-proteasome system is involved in the regulation of many biological processes in eukaryotic cells [31]. Polyubiquitin chains are formed after specific proteins are ubiquitinated [32, 33]. Proteins with polyubiquitin chains are then recognized by the proteasome and degraded [34]. This experiment showed that MG132 was able to up-regulate the expression of YAP in the siRNA treatment group, which indicated that the degradation of YAP might also be closely related to the ubiquitin-proteasome degradation pathway.

In addition, the ALP, Runx2, osteopontin, and osteocalcin expression levels in the osteoblasts were up-regulated in the co-cultured groups with FGFR2 mutations, suggesting that the C278F- and C342Y-FGFR2 mutations were also closely related to the osteoblast differentiation. Other studies have shown that the Hippo/YAP pathway exerted different effects on osteogenesis [35], but the specific molecular mechanism has not been clarified. We will also carry out further related studies to explore and reveal the underlying mechanism.

In conclusion, the Crouzon mutations (C278F- and C342Y-) of the dura cells alter the physiological regulation from the dura mater on osteoblasts. Our studies suggest that gain-of-function mutations of FGFR2 in the dura cells could enhance osteoblast proliferation and might influence the pathogenesis of craniosynostosis by affecting the Hippo/YAP-PI3K-AKT signaling pathway. While YAP interacts with multiple signaling pathways, the dual regulatory effects of YAP in different tissues make the regulatory mechanism more complex and complicated. Therefore, it is of great importance to further explore and elucidate the regulatory mechanism in the selection of therapeu-

tic targets for different diseases, including craniosynostosis.

Acknowledgements

This work was supported by the Special Research Fund for Plastic Surgery Hospital, Chinese Academy of Medical Sciences and Peking Union Medical College, number 1200418048, and the Fundamental Research Funds for Central Public Research Institutes of Peking Union Medical College, number 2018PT31051.

Disclosure of conflict of interest

None.

Address correspondence to: Xiao-Lei Jin, The Sixteenth Department of Plastic Surgery, Plastic Surgery Hospital, Chinese Academy of Medical Sciences & Peking Union Medical College (CAMS & PUMC), No. 33, Badachu Road, Shijingshan District, Beijing, China. Tel: +86-13911048536; E-mail: professor.jin@yahoo.com

References

[1] Boulet SL, Rasmussen SA and Honein MA. A population-based study of craniosynostosis in metropolitan Atlanta, 1989-2003. Am J Med Genet A 2008; 146A: 984-991.

[2] Coll G, El Ouadih Y, Abed Rabbo F, Jecko V, Sakka L and Di Rocco F. Hydrocephalus and Chiari malformation pathophysiology in FGFR2-related faciocraniosynostosis: a review. Neurochirurgie 2019; 65: 264-268.

[3] Azoury SC, Reddy S, Shukla V and Deng CX. Fibroblast growth factor receptor 2 (FGFR2) mutation related syndromic craniosynostosis. Int J Biol Sci 2017; 13: 1479-1488.

[4] Su N, Jin M and Chen L. Role of FGF/FGFR signaling in skeletal development and homeostasis: learning from mouse models. Bone Res 2014; 2: 14003.

[5] Merrill AE, Sarukhanov A, Krejci P, Idoni B, Camacho N, Estrada KD, Lyons KM, Deixler H, Robinson H, Chitayat D, Curry CJ, Lachman RS, Wilcox WR and Krakow D. Bent bone dysplasia-FGFR2 type, a distinct skeletal disorder, has deficient canonical FGF signaling. Am J Hum Genet 2012; 90: 550-557.

[6] Ang BU, Spivak RM, Nah HD and Kirschner RE. Dura in the pathogenesis of syndromic craniosynostosis: fibroblast growth factor receptor 2 mutations in dural cells promote osteogenic proliferation and differentiation of osteoblasts. J Craniofac Surg 2010; 21: 462-467.

[7] Ma S, Meng Z, Chen R and Guan KL. The hippo pathway: biology and pathophysiology. Annu Rev Biochem 2019; 88: 577-604.

[8] Misra JR and Irvine KD. The hippo signaling network and its biological functions. Annu Rev Genet 2018; 52: 65-87.

[9] Piccolo S, Dupont S and Cordenonsi M. The biology of YAP/TAZ: hippo signaling and beyond. Physiol Rev 2014; 94: 1287-1312.

[10] Lin KC, Park HW and Guan KL. Regulation of the hippo pathway transcription factor TEAD. Trends Biochem Sci 2017; 42: 862-872.

[11] Schick B, Wolf G, Romeike BF, Mestres P, Praetorius M and Plinkert PK. Dural cell culture. A new approach to study duraplasty. Cells Tissues Organs 2003; 173: 129-137.

[12] Moldovan GL, Pfander B and Jentsch S. PCNA, the maestro of the replication fork. Cell 2007; 129: 665-679.

[13] Boehm EM, Gildenberg MS and Washington MT. The many roles of PCNA in eukaryotic DNA replication. Enzymes 2016; 39: 231-254.

[14] Choe KN and Moldovan GL. Forging ahead through darkness: PCNA, still the principal conductor at the replication fork. Mol Cell 2017; 65: 380-392.

[15] Miraoui H and Marie PJ. Fibroblast growth factor receptor signaling crosstalk in skeletogenesis. Sci Signal 2010; 3: re9.

[16] Dailey L, Ambrosetti D, Mansukhani A and Basilico C. Mechanisms underlying differential responses to FGF signaling. Cytokine Growth Factor Rev 2005; 16: 233-247.

[17] Zhao B, Li L, Tumaneng K, Wang CY and Guan KL. A coordinated phosphorylation by Lats and CK1 regulates YAP stability through SCF(beta-TRCP). Genes Dev 2010; 24: 72-85.

[18] Alcon A, Metzler P, Eswarakumar J, Wilson AT and Steinbacher DM. Osteogenesis of Crouzon-mutated cells in an experimental model. J Craniofac Surg 2018; 29: 237-242.

[19] Chen H, Ma J, Li W, Eliseenkova AV, Xu C, Neubert TA, Miller WT and Mohammadi M. A molecular brake in the kinase hinge region regulates the activity of receptor tyrosine kinases. Mol Cell 2007; 27: 717-730.

[20] Chen L and Deng CX. Roles of FGF signaling in skeletal development and human genetic diseases. Front Biosci 2005; 10: 1961-1976.

[21] Marie PJ. Fibroblast growth factor signaling controlling osteoblast differentiation. Gene 2003; 316: 23-32.

[22] Warren SM, Greenwald JA, Nacamuli RP, Fong KD, Song HJ, Fang TD, Mathy JA and Longaker MT. Regional dura mater differentially regulates osteoblast gene expression. J Craniofac Surg 2003; 14: 363-370.

[23] Cooper GM, Durham EL, Cray JJ Jr, Siegel MI, Losee JE and Mooney MP. Tissue interactions

between craniosynostotic dura mater and bone. J Craniofac Surg 2012; 23: 919-924.
[24] Leach JP, Heallen T, Zhang M, Rahmani M, Morikawa Y, Hill MC, Segura A, Willerson JT and Martin JF. Hippo pathway deficiency reverses systolic heart failure after infarction. Nature 2017; 550: 260-264.
[25] Huang HL, Wang S, Yin MX, Dong L, Wang C, Wu W, Lu Y, Feng M, Dai C, Guo X, Li L, Zhao B, Zhou Z, Ji H, Jiang J, Zhao Y, Liu XY and Zhang L. Par-1 regulates tissue growth by influencing hippo phosphorylation status and hippo-salvador association. PLoS Biol 2013; 11: e1001620.
[26] Zheng Y and Pan D. The hippo signaling pathway in development and disease. Dev Cell 2019; 50: 264-282.
[27] He L, Yuan L, Yu W, Sun Y, Jiang D, Wang X, Feng X, Wang Z, Xu J, Yang R, Zhang W, Feng H, Chen HZ, Zeng YA, Hui L, Wu Q, Zhang Y and Zhang L. A regulation loop between YAP and NR4A1 balances cell proliferation and apoptosis. Cell Rep 2020; 33: 108284.
[28] Heinemann A, Cullinane C, De Paoli-Iseppi R, Wilmott JS, Gunatilake D, Madore J, Strbenac D, Yang JY, Gowrishankar K, Tiffen JC, Prinjha RK, Smithers N, McArthur GA, Hersey P and Gallagher SJ. Combining BET and HDAC inhibitors synergistically induces apoptosis of melanoma and suppresses AKT and YAP signaling. Oncotarget 2015; 6: 21507-21521.
[29] Lin Z, Zhou P, von Gise A, Gu F, Ma Q, Chen J, Guo H, van Gorp PR, Wang DZ and Pu WT. Pi3k-cb links Hippo-YAP and PI3K-AKT signaling pathways to promote cardiomyocyte proliferation and survival. Circ Res 2015; 116: 35-45.
[30] Meng Z, Moroishi T and Guan KL. Mechanisms of hippo pathway regulation. Genes Dev 2016; 30: 1-17.
[31] Nandi D, Tahiliani P, Kumar A and Chandu D. The ubiquitin-proteasome system. J Biosci 2006; 31: 137-155.
[32] Swatek KN and Komander D. Ubiquitin modifications. Cell Res 2016; 26: 399-422.
[33] Zheng N and Shabek N. Ubiquitin ligases: structure, function, and regulation. Annu Rev Biochem 2017; 86: 129-157.
[34] Mevissen TET and Komander D. Mechanisms of deubiquitinase specificity and regulation. Annu Rev Biochem 2017; 86: 159-192.
[35] Xiong J, Almeida M and O'Brien CA. The YAP/TAZ transcriptional co-activators have opposing effects at different stages of osteoblast differentiation. Bone 2018; 112: 1-9.